Synthesis and X-ray Crystal Structure of the Heterodinuclear Iron–Chromium Carbonyl Nitrosyl Anion Complex [*trans*-(η^5-MeCp)(CO)Fe(μ-CO)$_2$Cr(NO)-(η^5-Cp)][Ph_3PCH_3], Conversion to a Heterodinuclear Methoxycarbyne Complex, and Kinetics of Thermally-Induced Oxygen to Iron Methyl Migration

Bing Wang and William H. Hersh*

Department of Chemistry and Biochemistry, Queens College of the City University of New York, Flushing, New York 11367-1597

Arnold L. Rheingold†

Department of Chemistry and Biochemistry, University of Delaware, Newark, Delaware 19716

Received November 13, 1992

Reaction of MeCpFe(CO)$_2^-$Na$^+$ (MeCp = η^5-$CH_3C_5H_4$) with CpCr(CO)(NO)THF (Cp = η^5-C_5H_5) gives the heterodinuclear anion [MeCp(CO)Fe(μ-CO)$_2$Cr(NO)Cp]$^-$Na$^+$ (**1**), which was further characterized by conversion to the $(Ph_3P)_2N^+$ (**1-PPN$^+$**) and $Ph_3PCH_3^+$ (**1-$Ph_3PCH_3^+$**) salts. The X-ray crystal structure of **1-$Ph_3PCH_3^+$** (space group $P2_1/n$, a = 9.276(2) Å, b = 14.925(3) Å, c = 21.875(4) Å, β = 102.60(5)°, and R = 0.043, R_w = 0.052 for 6774 independent reflections) shows that it crystallizes as the trans isomer with a Fe–Cr single-bond distance of 2.611(1) Å and confirms the location of the terminal nitrosyl ligand on chromium. Alkylation with $CH_3OSO_2CF_3$ or [$(CH_3)_3O$][BF_4] gives the novel methoxycarbynes *cis*- and *trans*-MeCp-(CO)Fe(μ-COCH$_3$)(μ-CO)Cr(NO)Cp (**2c, 2t**) in low yield. The isomers are separable by column chromatography, although **2c** gives some **2t** at room temperature as both undergo slow decomposition. Thermal decomposition of **2t** occurs at a convenient rate at 50 °C in C_6D_6 to give MeCpFe(CO)$_2$CH$_3$ (**3**, 45%), CpCr(CO)$_2$(NO) (**4**, 20%), and [MeCpFe(CO)$_2$]$_2$ (48%) as the only soluble products. In the presence of PPh_3, MeCpFe(CO)(PPh_3)CH$_3$ (**3L**), CpCr(CO)-(NO)PPh_3 (**4L**), and **1-$Ph_3PCH_3^+$** also form. The decomposition of **2t** follows pseudo-first-order kinetics with a rate law $-d[\mathbf{2t}]/dt = (k_1 + k_2[PPh_3])\mathbf{2t}$, where k_1 corresponds to the thermal reaction in the absence of PPh_3 and the bimolecular k_2 path leads to **1-$Ph_3PCH_3^+$**. However, the yield of soluble products for the k_1 pathway declines with increasing PPh_3 concentration much faster than expected, suggesting the presence of an intermediate that is trapped by PPh_3. The product of this trapping reaction appears to be additional **1-$Ph_3PCH_3^+$**, and a mechanism that quantitatively fits the rate and product yield data is proposed. The oxygen to metal methyl migration reaction is only the second such reaction of a methoxycarbyne to be reported.

Introduction

We recently reported the first example of a new reaction in which the alkyl group of a bridging alkoxycarbyne ligand migrates from oxygen to one of the bridged metal atoms with formation of a mononuclear iron alkyl complex (eq 1).[1] Kinetic studies showed that the migration reactions

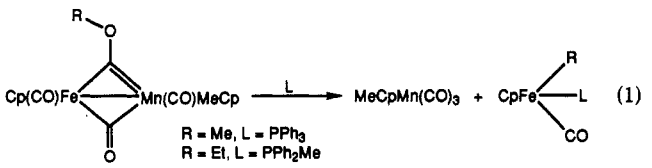

(1)

were independent of phosphine concentration, with the phosphine ligand serving simply to supply the necessary additional donor ligand following metal–metal bond cleavage.[2] In order to probe the generality, if any, of this reaction, we are interested in studying the chemistry of related carbyne complexes. While the choice of other metals could be made on an arbitrary basis, we wanted to investigate carbyne complexes for which we might be able to synthesize the isomeric *acyl* complexes with the same metals and ligands, since the above methyl migration reaction might serve as a mechanistic bridge between observable isomers if both were kinetically stable. We had previously synthesized the iron–molybdenum toluoyl complex[3]

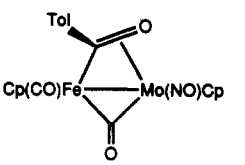

† Author to whom inquiries regarding the crystal structure should be made.

(1) (a) Fong, R. H.; Hersh, W. H. *Organometallics* **1985**, *4*, 1468–1470. (b) Fong, R. H.; Lin, C.-H.; Idmoumaz, H.; Hersh, W. H. *Ibid.* **1993**, *12*, 503–516.

(2) (a) Fong, R. H.; Hersh, W. H., manuscript in preparation. (b) Idmoumaz, H.; Lin, C.-H.; Hersh, W. H., manuscript in preparation.

0276-7333/93/2312-1319$04.00/0

but the simplest starting material for the carbyne synthesis, $CpMo(CO)(NO)THF$, apparently cannot be prepared by photolysis of $CpMo(CO)_2(NO)$. However, the chromium THF analog is known,[4] and so we decided to investigate its chemistry first. We describe here the synthesis and X-ray structure of a novel iron–chromium heterodinuclear anion, its conversion to cis and trans isomers of a novel methoxycarbyne complex, and kinetic studies on the oxygen to iron methyl migration reaction of this material, the second such alkoxycarbyne that exhibits this novel reaction.

Results

Synthesis of a Dinuclear Iron–Chromium Anion. Addition of $MeCpFe(CO)_2^-Na^+$ to a ~1:1 mixture of $CpCr(CO)_2NO$ and $CpCr(CO)(NO)THF$ in THF gave the desired heterodinuclear anion **1** as a brown-black solid in 59% yield, based on total chromium (eq 2). The infrared

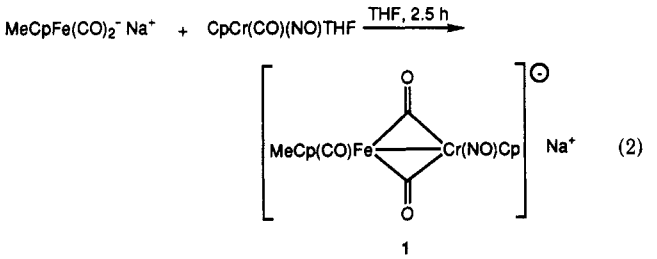

1

spectrum in THF is complicated by ion-pairing but exhibits a single band due to a terminal carbonyl ligand at 1894 cm^{-1}, bands due to bridging carbonyl ligands at 1746, 1718, 1672, and 1597 cm^{-1}, and a band due to a terminal nitrosyl ligand at 1557 cm^{-1}. In acetonitrile, where ion-pairing is evidently unimportant, three major bands are seen at 1891, 1698, and 1581 cm^{-1}. Metathesis of the Na^+ salt of **1** with PPN^+Cl^- (PPN^+ = bis(triphenylphosphine)nitrogen(+1)) gave the corresponding salt **1-PPN$^+$**, which exhibited an IR spectrum in THF (as well as in acetonitrile and methylene chloride) similar to that of the sodium salt in acetonitrile, confirming that the simplified spectrum results from the absence of ion-pairing. Metathesis of **1** with $Ph_3PCH_3^+Br^-$ gave the analogous salt **1-PPh$_3$PCH$_3^+$**. The IR bands due to the terminal FeCO and the bridging carbonyl ligands are similar to those seen for the FeMn anion $[Cp(CO)Fe(\mu\text{-}CO)_2Mn(CO)MeCp]^-PPN^+$ at 1899 and 1671 cm^{-1},[1] and about 100 cm^{-1} lower than those of the isoelectronic and isostructural iron dimer $[CpFe(CO)_2]_2$ at 1996 and 1773 cm^{-1}, due to the negative charge. The IR band due to the terminal CrNO ligand is similarly ~100 cm^{-1} lower than that of isoelectronic and isostructural *trans*-$[CpCr(NO)_2]_2$ at 1679 cm^{-1},[5] and is virtually the same as that of the radical anion $[CpCr(NO)_2]_2^-$.[6] At room temperature the ^1H NMR spectra of the Na^+ and PPN^+ salts of **1** exhibit broad peaks in CD_3CN solution, presumably indicating the presence of interconverting cis and trans isomers,[1] but in acetone-d_6 and CD_2Cl_2 relatively sharp spectra were obtained, indicating rapid isomerization and/or the presence of a single isomer for the two salts.

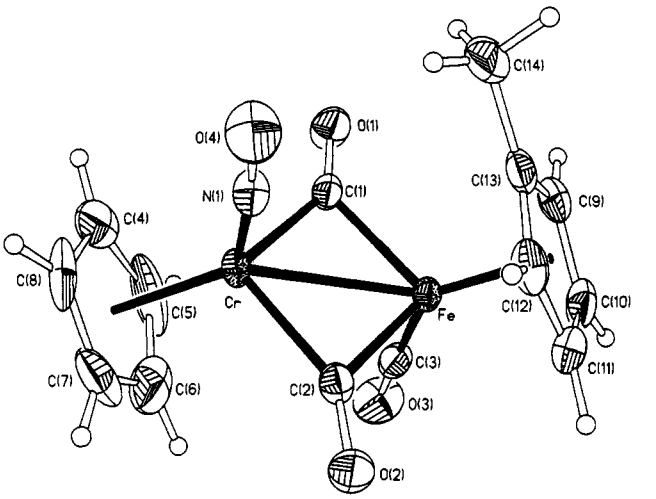

Figure 1. ORTEP drawing of the anion of **1-PPh$_3$CH$_3^+$**.

The $Ph_3PCH_3^+$ salt of **1** clearly exhibited two isomers in a ~30:70 ratio in CD_2Cl_2 at room temperature, however, and differences between cis/trans ratios of the PPN^+ and $Ph_3PCH_3^+$ salts of $[Cp(CO)Fe(\mu\text{-}CO)_2Mn(CO)MeCp]^-$ have been noted previously.[1b]

The ^{13}C NMR spectrum was recorded in acetone-d_6 at −48 °C in order to slow down any possible cis/trans isomerization, and in fact only a single set of peaks was observed. Signals for the terminal FeCO ligand at 214.7 ppm and the bridging carbonyl ligands at 320.1 ppm are in accord with the proposed structure, and the presence of only two CH peaks for the MeCp ring is in accord with the presence of a symmetry plane in the anion. The positions of the peaks are comparable to those in $[Cp(CO)Fe(\mu\text{-}CO)_2Mn(CO)MeCp]^-PPN^+$ at 216.4 and 302.8 ppm,[1b] while for comparison the CO peak in $CpCr(CO)_2NO$ was observed at 238.6 ppm, consistent with the absence of a terminal CrCO ligand in **1**.

The Na^+ salt of **1** is quite air-sensitive although not pyrophoric, decomposing to give large amounts of benzene-insoluble material and some $[MeCpFe(CO)_2]_2$ but no $CpCr(CO)_2NO$. The PPN^+ and $Ph_3PCH_3^+$ salts are air-stable for short periods of time as solids, while the PPN^+ salt was found to rapidly decompose in acetone solution in the air, giving material similar to that seen for the Na^+ salt. Most interestingly, both the PPN^+ and $Ph_3PCH_3^+$ salts decompose on standing in methylene chloride overnight under a nitrogen atmosphere to give $[MeCpFe(CO)_2]_2$, a small amount of $CpCr(CO)_2NO$, and a black paramagnetic chromium compound having a single nitrosyl band in the IR spectrum at ~1640 cm^{-1}. This material is likely to be related to paramagnetic 17-electron chromium nitrosyl compounds characterized by Legzdins,[6,7] and in particular could be the same as the uncharacterized reduction product of $CpCr(NO)_2Cl$,[6] on the basis of color (dark brown), solubility in CH_2Cl_2, and IR; work is in progress to determine its identity.

X-ray Structure of 1-Ph$_3$PCH$_3^+$. Crystals of **1-PPN$^+$** and **1-Ph$_3$PCH$_3^+$** suitable for X-ray structure determinations were obtained from acetonitrile and acetonitrile/ether solution, respectively. The anion of the PPN^+ salt was disordered with respect to the iron and chromium atoms, despite the presence of the methylcyclopentadienyl ligand, but no such difficulties were encountered with the anion of the $Ph_3PCH_3^+$ salt, perhaps due to the smaller cation. The molecular structure of the anion is shown in Figure 1, atomic coordinates and isotropic thermal

(3) Bonnesen, P. V.; Baker, A. T.; Hersh, W. H. *J. Am. Chem. Soc.* **1986**, *108*, 8304–8305.
(4) Hames, B. W.; Legzdins, P.; Martin, D. T. *Inorg. Chem.* **1978**, *17*, 3644–3647.
(5) Kirchner, R. M.; Marks, T. J.; Kristoff, J. S.; Ibers, J. A. *J. Am. Chem. Soc.* **1973**, *95*, 6602–6613.
(6) Legzdins, P.; Wassink, B. *Organometallics* **1984**, *3*, 1811–1817.

Table I. Atomic Coordinates (×10⁴) and Equivalent Isotropic Displacement Coefficients (Å² × 10³)

	x	y	z	U(eq)[a]
Cr	2911(1)	6680(1)	674(1)	30(1)
Fe	5185(1)	7665(1)	591(1)	29(1)
P	1811(1)	2727(1)	1497(1)	34(1)
N(1)	1610(3)	7475(2)	569(1)	39(1)
O(1)	3765(3)	6830(2)	-575(1)	57(1)
O(2)	4730(3)	7490(2)	1851(1)	55(1)
O(3)	7345(3)	6238(2)	781(2)	67(1)
O(4)	579(3)	7992(2)	507(2)	64(1)
C(1)	3820(4)	6965(2)	-36(2)	34(1)
C(2)	4360(4)	7312(2)	1309(2)	35(1)
C(3)	6460(4)	6800(2)	706(2)	38(1)
C(4)	1972(7)	5388(3)	304(2)	72(2)
C(5)	3492(7)	5264(3)	516(3)	84(3)
C(6)	3816(6)	5413(3)	1140(3)	83(2)
C(7)	2567(8)	5621(3)	1329(2)	74(2)
C(8)	1431(5)	5600(3)	821(3)	67(2)
C(9)	5679(4)	8652(3)	-42(2)	46(1)
C(10)	6755(4)	8646(3)	524(2)	50(1)
C(11)	6068(5)	8878(3)	1015(2)	49(1)
C(12)	4555(5)	9005(2)	753(2)	48(1)
C(13)	4308(4)	8869(2)	97(2)	46(1)
C(14)	2883(5)	8978(3)	-368(2)	74(2)
C(15)	3605(4)	2647(2)	2003(2)	34(1)
C(16)	4869(5)	2786(3)	1775(2)	55(2)
C(17)	624495)	2687(4)	2181(2)	71(2)
C(18)	6354(5)	2450(3)	2789(2)	57(2)
C(19)	5107(5)	2319(3)	3017(2)	51(1)
C(20)	3722(4)	2409(2)	2629(2)	40(1)
C(21)	982(4)	1637(2)	1465(2)	38(1)
C(22)	1241(5)	1011(3)	1032(2)	61(2)
C(23)	760(5)	139(3)	1054(3)	80(2)
C(24)	27(6)	-112(3)	1508(3)	79(2)
C(25)	-271(6)	496(4)	1923(2)	80(2)
C(26)	198(6)	1382(3)	1904(2)	62(2)
C(27)	737(4)	3552(2)	1791(2)	37(1)
C(28)	-707(4)	3689(3)	1460(2)	52(1)
C(29)	-1523(5)	4367(3)	1638(2)	64(2)
C(30)	-929(6)	4899(3)	2146(3)	67(2)
C(31)	494(6)	4758(3)	2480(2)	59(2)
C(32)	1336(5)	4089(2)	2301(2)	46(1)
C(33)	1933(5)	3067(3)	725(2)	53(2)

[a] Equivalent isotropic U defined as one third of the trace of the orthogonalized U_{ij} tensor.

parameters are given in Table I, and selected bond lengths and angles are given in Table II. Principal features include (1) the trans geometry of the cyclopentadienyl ligands, (2) the location of the nitrosyl ligand on chromium, and (3) the normal (vide infra) Fe–Cr bond length of 2.611 (1) Å. The geometry of the μ-CO ligands is interesting in that the M–C bond lengths exhibit C_2 point-group symmetry despite the fact that both CO vectors are tipped toward the iron atom:

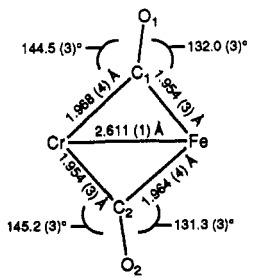

That is, the Cr–C(1) and Fe–C(2) bond lengths are equivalent (average 1.966(4) Å) to each other despite the different metal atoms, as are the Cr–C(2) and Fe–C(1)

Table II. Selected Bond Lengths (Å) and Bond Angles (deg)

Cr–Fe	2.611(1)	Cr–N(1)	1.672(3)
Cr–C(1)	1.968(4)	Cr–C(2)	1.954(3)
Cr–C(4)	2.196(5)	Cr–C(5)	2.226(5)
Cr–C(6)	2.224(5)	Cr–C(7)	2.203(5)
Cr–C(8)	2.185(5)	Fe–C(1)	1.954(3)
Fe–C(2)	1.964(4)	Fe–C(3)	1.732(4)
Fe–C(9)	2.139(4)	Fe–C(10)	2.092(4)
Fe–C(11)	2.115(4)	Fe–C(12)	2.134(4)
Fe–C(13)	2.162(4)	N(1)–O(4)	1.213(4)
O(1)–C(1)	1.186(4)	O(2)–C(2)	1.189(4)
O(3)–C(3)	1.159(5)	Cr–CNT1[a]	1.877
Fe–CNT2[b]	1.759		

Fe–Cr–N(1)	99.2(1)	Fe–Cr–C(1)	48.0(1)
N(1)–Cr–C(1)	99.1(2)	Fe–Cr–C(2)	48.4(1)
N(1)–Cr–C(2)	96.8(1)	C(1)–Cr–C(2)	96.3(1)
Cr–Fe–C(1)	48.5(1)	Cr–Fe–C(2)	48.0(1)
C(1)–Fe–C(2)	96.4(1)	Cr–Fe–C(3)	96.1(1)
C(1)–Fe–C(3)	91.2(1)	C(2)–Fe–C(3)	93.3(2)
Cr–N(1)–O(4)	173.9(3)	Cr–C(1)–Fe	83.4(1)
Cr–C(1)–O(1)	144.5(3)	Fe–C(1)–O(1)	132.0(3)
Cr–C(2)–Fe	83.6(1)	Cr–C(2)–O(2)	145.2(3)
Fe–C(2)–O(2)	131.3(3)	Fe–C(3)–O(3)	178.0(3)
Fe–Cr–CNT(1)[a]	133.9	N(1)–Cr–CNT(1)[a]	126.8
C(1)–Cr–CNT(1)[a]	116.0	C(2)–Cr–CNT(1)[a]	116.1
Cr–Fe–CNT(2)[b]	135.2	C(1)–Fe–CNT(2)[b]	120.6
C(2)–Fe–CNT(2)[b]	118.7	C(3)–Fe–CNT(2)[b]	128.7

[a] CNT(1) is the centroid of atoms C(4)–C(8). [b] CNT(2) is the centroid of atoms C(9)–C(13).

bond lengths (1.954(3) Å), while the Cr–(μ-C)–O angles average 144.9(4)° but the Fe–(μ-C)–O angles average only 131.7(4)°. The Fe(μ-CO)$_2$Cr core of the anion is nearly planar, with the carbonyl ligands tipped toward the terminal CO ligand with a C(1)–Fe–Cr–C(2) dihedral angle of 174.9°. The trans CO and NO ligands are essentially coplanar as well, with a C(3)–Fe–Cr–N dihedral angle of 180°.

Synthesis of Iron–Chromium Methoxycarbynes. Alkylation of **1** to give the new methoxycarbynes **2c** and **2t** could be accomplished by reaction with $MeOSO_2CF_3$, but only gave yields of ~3% each, in contrast to the much higher yield alkylation of the related FeMn anion.[1] The major product was a brown benzene-insoluble paramagnetic material that may be related to that described above derived from **1**-**PPN**$^+$ and **1**-**Ph$_3$PCH$_3$**$^+$ and CH_2Cl_2, but we have been unable to characterize it. Substantially better yields, 10% each of **2t** and **2c**, were obtained with $Me_3O^+BF_4^-$ (eq 3). The major soluble reaction product

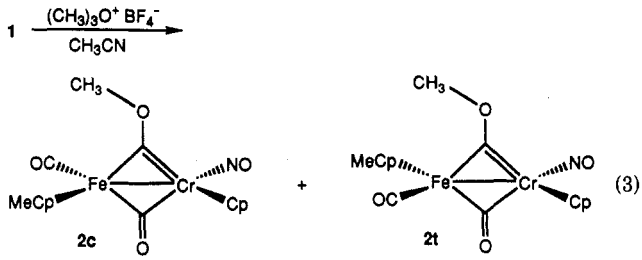

was [MeCpFe(CO)$_2$]$_2$ (64%), and it provides the reason for the use of the methylcyclopentadienyl complex: when we initially examined this chemistry using the biscyclopentadienyl system, we found that the carbyne products and the [CpFe(CO)$_2$]$_2$ byproduct could not be separated by column chromatography, and so switched to the MeCp iron anion since in this case the separation would be of the Cp/MeCp carbynes and the bis(methylcyclopentadienyliron) dimer [MeCpFe(CO)$_2$]$_2$. While the separation was still nontrivial, it could be accomplished. In addition to the above products, once again a benzene-insoluble brown

(7) (a) Legzdins, P.; Nurse, C. R. *Inorg. Chem.* **1985**, *24*, 327–332. (b) Herring, F. G.; Legzdins, P.; Mcneil, W. S.; Shaw, M. J.; Batchelor, R. J.; Einstein, F. W. B. *J. Am. Chem. Soc.* **1991**, *113*, 7049–7050.

Scheme I

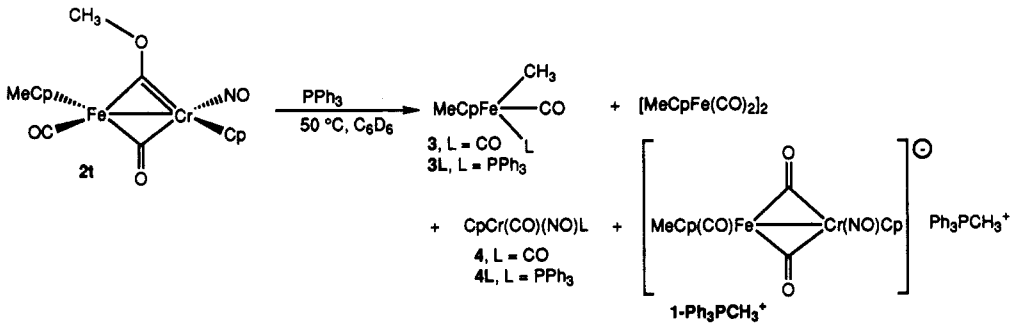

powder, which is presumably related to that formed in the methyl triflate reaction, was isolated but again could not be characterized.

The two carbyne products **2c** and **2t** were separated by chromatography and characterized by IR, ^{1}H NMR, and ^{13}C NMR. Suitable elemental analyses could not be obtained despite repeated attempts, presumably due to the limited thermal stability of the carbynes (vide infra). Similarly, mass spectrometry (electron ionization) failed to give any significant ions due to the carbynes or any heterodinuclear fragment ions; instead the mass spectrum consisted primarily of peaks due to $[MeCpFe(CO)_2]_2$, as well as less intense peaks at 117 and 147 that may be due to CpCr and CpCr(NO), respectively. The isomers are presumed to be cis and trans isomers as shown, and the more polar isomer—that which is eluted second of the two—is presumed to be the cis isomer by analogy to the polarity of $[CpFe(CO)_2]_2$[5,8] and by analogy to other separations of cis/trans isomers.[3,9] The arrangement of carbonyl and nitrosyl ligands is supported by the IR and ^{13}C NMR spectra. The cis isomer, for instance, has a terminal FeCO band at 1966 cm^{-1}, a bridging CO band at 1794 cm^{-1}, and a terminal CrNO band at 1659 cm^{-1}; for comparison, the FeMn methoxycarbyne MeCp(CO)Fe(μ-$COCH_3$)(μ-CO)Mn(CO)Cp has FeCO and bridging carbonyl bands at 1950 and 1767 cm^{-1},[1b] and $[CpCr(NO)_2]_2$ has a terminal CrNO band at 1679 cm^{-1}, as noted above.[5] The ^{13}C NMR spectra were recorded at 0 °C to prevent complications due to thermal decomposition. The principal feature for both isomers (which differ by ~1–2 ppm for each peak) is the confirmation of the presence of the carbyne moiety, as judged by the downfield peak at ~428 ppm due to the carbyne carbon itself and the methoxy peak at ~73 ppm. Other peaks of interest include a somewhat broad peak at ~290 ppm due to the bridging carbonyl ligand, the terminal FeCO band at ~212 ppm, and the separate resonances for the four diastereotopic CH carbons of the MeCp ring, consistent with the loss of the plane of symmetry present in **1** due to the incorporation of the methoxy group. The peak positions are comparable to those we have reported for MeCp(CO)Fe(μ-$COCH_3$)(μ-CO)Mn(CO)Cp,[1] the major differences being that the bridging carbons in the FeMn compound are observed at higher field, at 391 (carbyne) and 273 (μ-CO) ppm. A similar downfield shift for the FeCr compound compared to the FeMn compound was seen for the anions above and may be attributable to the presence of the π-acid NO ligand on chromium. The reason for the broadness of the μ-CO carbon, particularly in **2t**, is not known, and there is no evidence from our other ^{13}C NMR spectra of broadening due to quadrupolar coupling to Cr or N or from ^{1}H NMR or IR spectra of any other fluctional process that might (for instance) exchange this carbonyl with the NO ligand. The ^{1}H NMR spectra exhibit methoxy singlets for each isomer near 4.3 ppm, four separate resonances for the diastereotopic MeCp cyclopentadienyl hydrogens in **2c**, and three separate signals—two resonances overlap—for these hydrogens in **2t**, as well as the expected CpCr and *Me*CpFe singlets.

Thermal Reactions of Methoxycarbyne 2. Decomposition of both carbynes was observed at room temperature, **2t** with a half-life of ~12 h ($k \approx 1.6 \times 10^{-5}$ s^{-1}) and **2c** with a half-life of ~10 h ($k \approx 1.8 \times 10^{-5}$ s^{-1}). While no trace of **2c** was observed during the decomposition of **2t**, significant amounts of **2t** formed during the decomposition of **2c**: after 2 h, the ratio of **2t**:**2c** was ~15:85, and this increased to ~25:75 as the decomposition neared completion. The two reactions gave the same final products and in similar yields, namely the methyl migration product $MeCpFe(CO)_2CH_3$ (**3**, ~40%), $[MeCpFe(CO)_2]_2$ (51% from **2t** and 66% from **2c**), and $CpCr(CO)_2NO$ (**4**, ~23%). Subsequent experiments were carried out with **2t** to avoid the complication of isomerization seen with **2c**.

Decomposition of **2t** occurred at a convenient rate at 50 °C in C_6D_6 and was observed by ^{1}H NMR both in the presence and absence of PPh_3. All products (Scheme I, Table III) were identified by ^{1}H NMR by comparison of spectra to those of independently prepared compounds. Three iron compounds were observed, including both $MeCpFe(CO)_2CH_3$ (**3**) and $MeCpFe(CO)(PPh_3)CH_3$ (**3L**) formed by oxygen to iron methyl migration and $[MeCpFe(CO)_2]_2$. Two chromium compounds were observed, namely $CpCr(CO)_2NO$ (**4**) and $CpCr(CO)(NO)PPh_3$ (**4L**).[10] In a control experiment (eq 4), less than 0.5% conversion

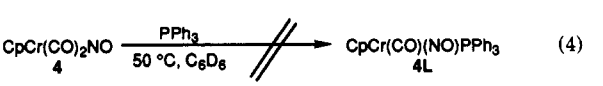

(4)

of **4** to **4L** occurred in 2.3 h at 50 °C in the presence of 0.1 M PPh_3 (using a 5:1 ratio of PPh_3/**4**), obviously far too little to account for the presence of **4L** in the carbyne reactions, which approached completion in less than 1 h. Thus, **4L** is a primary product of the carbyne reaction, and similarly **3** and **3L** are known not to interconvert under

(8) (a) Gansow, O. A.; Burke, A. R.; Vernon, W. D. *J. Am. Chem. Soc.* **1972**, *94*, 2550–2552. (b) Bullitt, J. G.; Cotton, F. A.; Marks, T. J. *Inorg. Chem.* **1972**, *11*, 671–676. (c) Adams, R. D.; Cotton, F. A. *J. Am. Chem. Soc.* **1973**, *95*, 6589–6594.

(9) Casey, C. P.; Fagan, P. J.; Miles, W. H. *J. Am. Chem. Soc.* **1982**, *104*, 1134–1136.

(10) Brunner, H. *J. Organomet. Chem.* **1969**, *16*, 119–124.

(11) (a) Treichel, P. M.; Shubkin, R. L.; Barnett, K. W.; Reichard, D. *Inorg. Chem.* **1966**, *5*, 1177–1181. (b) Su, S. R.; Wojcicki, A. *J. Organomet. Chem.* **1971**, *27*, 231–240.

Table III. Yield and Rate Constant Data for Thermal Decomposition of 2t

	[PPh_3]					
product	0	0.0097	0.032	0.063	0.49	0.83
$CpCr(CO)_2NO$ (4)	19.9 ± 0.8	36 ± 4	38 ± 2	31 ± 2	14.3 ± 0.8	7.8 ± 0.6
$CpCr(PPh_3)(CO)NO$ (4L)		40 ± 3	21 ± 1	8.8 ± 0.9	3.1 ± 0.4	3.0 ± 0.4
4:4L		48:52	65:35	78:22	82:18	72:28
$[MeCpFe(CO)_2]_2$	48 ± 3	51 ± 6	22 ± 3	10 ± 3	0 ± 1	3 ± 1
$MeCpFe(CO)(PPh_3)Me$ (3L)		28 ± 4	33 ± 2	22 ± 2	5.4 ± 0.5	1.9 ± 0.4
$MeCpFe(CO)_2Me$ (3)	45 ± 1	16 ± 3	5 ± 1	5.0 ± 0.9	0 ± 0.5	1.6 ± 0.3
3L:3		63:37	87:13	81:19	100:0	55:45
total Cr	19.9 ± 0.8[a]	76 ± 5	58 ± 2	40 ± 2	17.4 ± 0.9	10.8 ± 0.7
total FeMe	45 ± 1	44 ± 4	37 ± 2	27 ± 2	5.4 ± 0.5	3.5 ± 0.4
total Fe	93 ± 3	96 ± 7	60 ± 3	36 ± 4	5 ± 1	6 ± 1
anion (upper limit)[b]	0	4 ± 7	40 ± 3	60 ± 2	82.6 ± 0.9	89.2 ± 0.7
rate constant[c]	6.34 ± 0.05	6.81 ± 0.14	6.43 ± 0.12	7.11 ± 0.16	9.74 ± 0.17	11.92 ± 0.13

[a] This value was not used in Figure 4. [b] **1-$Ph_3PCH_3^+$**, assumed to be 0% in the absence of PPh_3 and at most 100 – % yield of the higher of total Cr or total Fe in the presence of PPh_3. [c] First-order rate of decomposition of **2t** × 10^4, s^{-1}, in C_6D_6 at 50 °C.

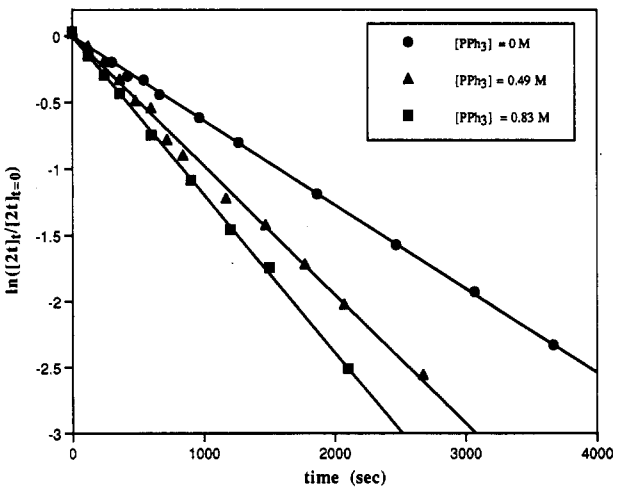

Figure 2. Representative first-order plots of the disappearance of **2t** in C_6D_6 at 50 °C.

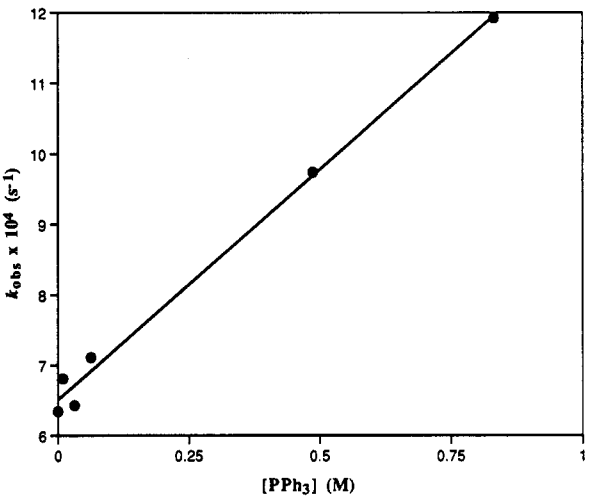

Figure 3. Plot of k_{obs} vs [PPh_3] (M) for the disappearance of **2t** in C_6D_6 at 50 °C.

such mild conditions.[2a,11] In addition to **3**, **3L**, **4**, **4L**, and the iron dimer, large amounts of precipitate formed in these reactions of **2t**, particularly at the highest concentrations of PPh_3. Isolation of this material showed it to be pure **1-$PPh_3CH_3^+$**, as judged by IR and ^1H NMR; that is, the precipitate was completely soluble in methylene chloride, and none of the uncharacterized paramagnetic compounds with the terminal NO band at ~1640 cm^{-1} were observed. Lastly, the reaction is not stoichiometric with respect to the methoxycarbyne CH_3 group: only about half of the alkyl not accounted for by formation of **1-$PPh_3CH_3^+$** was accounted for by **3** and **3L**. The fate of the missing CH_3 group is unknown. For instance, no methane was observed, despite the fact that small amounts would be readily observed under the sealed-tube conditions used.[1b] In principle, this question could be addressed by investigation of deuterium or ^{13}C-labeled analogs of **2t**, but in practice, due to the synthetic difficulty of the preparation of **2t** as well as the suspicion that intractable chromium decomposition products might still mask the labeled CH_3, no such attempts were made.

Kinetics of Decomposition of 2t. The reactions of **2t** in C_6D_6 at 50 °C were monitored by ^1H NMR spectroscopy, and under pseudo-first-order conditions (≥5-fold excess of PPh_3, with the exception of the 0.0097 M reaction where a ~3-fold excess was used), linear plots of ln [**2t**] vs time (Figure 2) were obtained to greater than three half-lives. Rate constants and product yields are collected in Table III. While the yield of **1-$PPh_3CH_3^+$** cannot be measured directly, an upper limit can be established by assuming that any Cr or Fe unaccounted for is tied up in the insoluble anion; at [PPh_3] = 0, the anion yield is assumed to be zero, at the next two concentrations the iron yield is highest and so was used to calculate the anion yield, while at the three highest phosphine concentrations, the chromium recovery is highest and so its yields were used to calculate the anion yield. A plot of the observed rate constants k_{obs} as a function of PPh_3 concentration is shown in Figure 3 and is linear from 0 to ~0.8 M PPh_3 with a non-zero intercept that gives essentially the same rate constant as that observed in the absence of PPh_3. The derived rate law is given in eq 5.

$$\frac{-d[2t]}{dt} = (k_1 + k_2[PPh_3])[2t] \qquad (5)$$

$k_1 = (6.51 \pm 0.10) \times 10^{-4}\ s^{-1}$,

$k_2 = (6.55 \pm 0.26) \times 10^{-4}\ M^{-1}\ s^{-1}$

Most interestingly, despite the ~2-fold increase in the decomposition rate constant k_{obs} over the phosphine concentration range investigated, the yield of soluble products declined to ~10%. For instance, even at low phosphine concentration (0.06 M), where the rate was only ~10% higher than in the absence of PPh_3, the yields of soluble products (i.e., total Cr and total Fe in Table III) were only ~40%, rather than the 90% expected if 10%

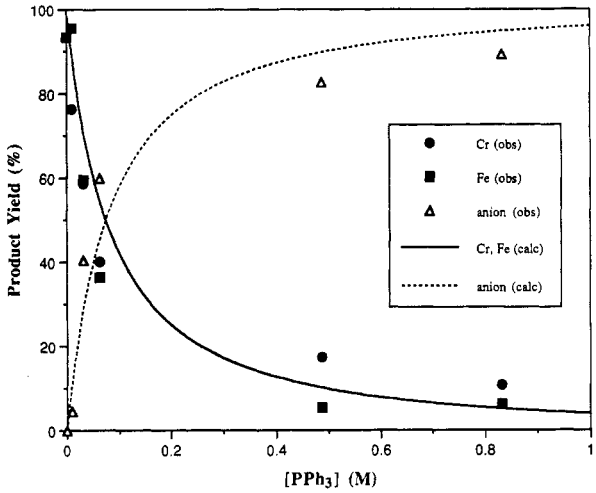

Figure 4. Observed and calculated product yields from the decomposition of **2t** as a function of PPh_3 concentration (M) at 50 °C in C_6D_6. The observed products are **3** + **3L** + $[MeCpFe(CO)_2]_2$ (Fe), **4** + **4L** (Cr), and the upper limit of **1-PPh$_3$CH$_3^+$** (anion), taken as the lesser of 100 − Fe or 100 − Cr. Theoretical curves were generated as described in the Discussion from eqs 7 and 8 using the rate constants shown in Scheme II.

of the carbyne was diverted to anion by a bimolecular pathway. A plot of product yields, given as total iron and total chromium, as well as the estimated anion yield as described above, is shown in Figure 4 as a function of $[PPh_3]$; the curves shown are calculated yields as will be described below. Clearly the yields appear to level off at high phosphine concentration, suggesting some type of saturation kinetics scheme, where phosphine traps a steady-state intermediate that is in equilibrium with starting material, and in this case diverts the intermediate from continuing on to soluble products to instead give more **1-PPh$_3$CH$_3^+$**.

Discussion

Anion **1** and our previously reported anion $[Cp(CO)Fe(\mu\text{-}CO)_2Mn(CO)MeCp]^-$ appear to be the only examples of biscyclopentadienyl heterodinuclear anions, so **1** is the first of this class of compounds for which the X-ray crystal structure has been solved; examples of *homo*nuclear biscyclopentadienyl anions and some of their structures have been reported, however, namely, Bergman's cobalt and rhodium dimers $[(\eta^5\text{-}C_5R_5)M(CO)]_2^n$ (M = Co, R = H, n = −1; M = Rh, R = Me, n = −1, −2).[12]

The number of Fe–Cr heteronuclear compounds appears to be relatively small,[13] and the number of examples that have been structurally characterized smaller yet. Data is collected in Table IV for these examples, along with the neutral homonuclear dimers $[CpFe(CO)_2]_2$, $[CpCr(NO)_2]_2$, and $[CpCr(CO)_3]_2$. Metal–metal bond lengths for the previously characterized Fe–Cr compounds range from 2.815(3) Å to 2.956(7) Å, all considerably longer than that of 2.611(1) Å in **1**. As a point of calibration, the Fe–CO bond lengths are also listed, and with the exception of the $AsMe_2$-bridged complex (which suffers from a disorder problem) are similar to the 1.73 Å bond length seen in **1**. None of these other Fe–Cr compounds have bridging carbonyl ligands, and only one has bridging ligands—μ-$AsMe_2$—of any kind, factors that tend to shorten the metal–metal bond length as has been well-documented for the Mn–Mn bond.[21] The long bond lengths are likely the result of steric strain due to the relatively high coordination number of chromium,[16,20] an effect that is readily appreciated by comparison of the pentacarbonyl complex $Cp(CO)_2FeCr(CO)_3Cp$ and the hexacarbonyl dimer $[CpCr(CO)_3]_2$ whose metal–metal bond is nearly 0.4 Å longer. These two examples also illustrate the fact that the relative shortness of the Fe–Cr bond in **1** is not accounted for simply by the presence of cyclopentadienyl ligands. As a final point, the Cr–CO bond lengths are ~0.12 Å longer than the Fe–CO bond lengths, presumably also due to steric strain due to the higher coordination number.

The most relevant comparisons are not with the heteronuclear compounds, but rather with the isoelectronic and isostructural dimers $[CpFe(CO)_2]_2$ and $[CpCr(NO)_2]_2$. The iron dimer Fe–Fe bond length of 2.534(2) Å is ~0.08 Å shorter, while the Cr–Cr bond length of 2.615(1) Å of the chromium dimer is virtually the same, as the Fe–Cr bond in **1**. If one ignores the different bridging ligands in these dimers, one might speculate that a neutral Fe–Cr doubly-bridged analog should have a Fe–Cr bond length of ~2.57 Å, so the negative charge in **1** has the effect of causing a very slight lengthening in the metal–metal bond length. In fact, the bridging ligands exhibit bond lengths that correlate with the M–M bond length rather than charge or the identity of bridging atom in these three compounds, so the above "neutral" Fe–Cr bond length is a reasonable estimate. On the other hand, the terminal Fe–CO and Cr–NO bond lengths do appear to be sensitive to charge, both being shorter in anionic **1** perhaps due to stronger π-back-bonding.

Alkylation of **1** is not as successful as that of the FeMn heterodinuclear anion.[1] The FeCr anion may be less nucleophilic due to the presence of the strong π-acid nitrosyl ligand. It is interesting to note that alkylation of the FeMn anion failed with $Me_3O^+BF_4^-$,[1b] and we presume that the success with the apparently less nucleophilic anion may be a consequence of ion-pairing[22] with this ionic reagent, with the relative failure of methyl triflate being due to the absence of ion-pairing. In addition to the lower nucleophilicity, the propensity of chromium nitrosyls to give paramagnetic 17-electron complexes evidently provides a low activation energy side reaction. For instance, one-electron oxidation followed by simple homolytic cleavage would give 17-electron $MeCpFe(CO)_2$, which would dimerize, and 17-electron $CpCr(CO)(NO)$, which presumably gives rise to the high yield of uncharacterized

(12) (a) Schore, N. E.; Ilenda, C. S.; Bergman, R. G. *J. Am. Chem. Soc.* **1977**, *99*, 1781–1787. (b) Krause, M. J.; Bergman, R. G. *Organometallics* **1986**, *5*, 2097–2108.

(13) Roberts, D. A.; Geoffroy, G. L. In *Comprehensive Organometallic Chemistry*; Wilkinson, G., Ed.; Pergamon Press: Oxford, 1982; Vol. 6; pp 763–877.

(14) Bryan, R. F.; Greene, P. T. *J. Chem. Soc. A* **1970**, 3064–3068.

(15) Calderón, J. L.; Fontana, S.; Frauendorfer, E.; Day, V. W. *J. Organomet. Chem.* **1974**, *64*, C10–C12.

(16) Huttner, G.; Mohr, G.; Friedrich, P. *Z. Naturforsch. B* **1978**, *33B*, 1254–1256.

(17) Vahrenkamp, H.; Keller, E. *Chem. Ber.* **1979**, *112*, 1991–1998.

(18) Herrmann, W. A.; Rohrmann, J.; Herdtweck, E.; Hecht, C.; Ziegler, M. L.; Serhadli, O. *J. Organomet. Chem.* **1986**, *314*, 295–305.

(19) Arndt, L. W.; Darensbourg, M. Y.; Delord, T.; Bancroft, B. T. *J. Am. Chem. Soc.* **1986**, *108*, 2617–2627.

(20) Adams, R. D.; Collins, D. E.; Cotton, F. A. *J. Am. Chem. Soc.* **1974**, *96*, 749–754.

(21) Creswick, M.; Bernal, I.; Reiter, B.; Herrmann, W. A. *Inorg. Chem.* **1982**, *21*, 645–652.

(22) Loupy, A.; Tchoubar, B.; Astruc, D. *Chem. Rev.* **1992**, *92*, 1141–1165.

Table IV. Comparison of Bond Lengths in Compounds with Fe–Cr, Fe–Fe, and Cr–Cr Bonds

compd	M–M	Fe–(μ-CO)	Cr–(μ-CO)	Fe–CO	Cr–NO	ref
1-$PPh_3CH_3^+$	2.611(1)	1.959(5)	1.961(7)	1.732(4)	1.672(3)	this work
trans-$Cp(CO)Fe(\mu\text{-}CO)_2Fe(CO)Cp$	2.534(2)	1.914(4)		1.748(6)		14
trans-$Cp(NO)Cr(\mu\text{-}NO)_2Cr(NO)Cp$	2.615(1)		1.960(3)[a]		1.690(3)	15
$(CO)_6Fe_2Cr(CO)_5(\mu_3\text{-}PPh)$	2.815(3)			1.75(3)	1.875(20)[b]	16
$(CO)_3Fe(\mu\text{-}AsMe_2)_2Cr(CO)_4$	2.829(3)			1.82(2)	1.82(2)[b]	17
$Cp(CO)_2FeCr(CO)_3Cp$	2.901(1)			1.748(5)	1.84(2)[b]	18
$(CO)_4FeCr(CO)_5^{2-}$	2.941(2)			1.74(2)	1.86(3)[b]	19
$H(CO)_4FeCr(CO)_5^-$	2.956(7)			1.76(2)	1.88(4)[b]	19
$Cp(CO)_3CrCr(CO)_3Cp$	3.281(1)				1.86(1)[b]	20

[a] Cr–(μ-NO). [b] Cr–CO.

Scheme II

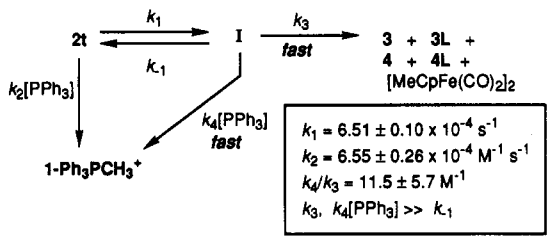

paramagnetic compound. Even for the FeMn anion, oxidation to give $[CpFe(CO)_2]_2$ and $MeCpMn(CO)_3$ occurred, albeit nonstoichiometrically due to the presence of only four CO ligands in the starting material, so perhaps it is not surprising to see an increase in the metal–metal bond cleavage reaction in a case where both metals can give rise to stable products without needing an additional two-electron donor ligand.

We have now examined the kinetic decomposition behavior of three alkoxycarbynes. The methoxycarbyne $Cp(CO)Fe(\mu\text{-}COCH_3)(\mu\text{-}CO)Mn(CO)MeCp$ undergoes thermal decomposition in the presence of PPh_3 by two parallel reactions, one simple first-order decomposition to $MeCpMn(CO)_3$ and a 16-electron fragment ($CpFe(CO)CH_3$ or more speculatively $CpFe{\equiv}COCH_3$[2a,23]) and the other bimolecular S_N2 attack of PPh_3 on the methoxy methyl group to give the Ph_3PMe^+ salt of the anion $[Cp(CO)Fe(\mu\text{-}CO)_2Mn(CO)MeCp]^-$. The yields of thermal decomposition products drop linearly with phosphine concentration as expected.[2a] The ethoxycarbyne $Cp(CO)Fe(\mu\text{-}COCH_2CH_3)(\mu\text{-}CO)Mn(CO)MeCp$ does not react with PPh_2Me by the dealkylation route, so its rate of decomposition is completely independent of phosphine concentration and product yields remain high.[2b] The mechanism of decomposition of **2t** is superficially identical to that of the FeMn methoxycarbyne with PPh_3, on the basis of their identical rate laws. However, as noted above, the yields of soluble iron and chromium products do not decrease linearly with $[PPh_3]$ as would be expected given a simple bimolecular side reaction involving S_N2 attack of PPh_3 on **2t** to give **1-$PPh_3CH_3^+$**.

The proposed kinetic scheme to account for the rate of disapperance of **2t** and appearance of products is shown in Scheme II. The major problem is to find rate constants that will give the linear disappearance of **2t** (Figure 3), and the nonlinear appearance of products (Figure 4) with $[PPh_3]$. The leveling off in yield suggests the presence of an intermediate (**I**), which is partitioned into a nonphosphine-dependent decomposition pathway (k_3) to give the soluble products and a phosphine-dependent pathway ($k_4[PPh_3]$) to give insoluble—that is, undetectable by ^1H NMR in C_6D_6—material. The product of this phosphine-dependent pathway is apparently **1-$PPh_3CH_3^+$** since all of the benzene-insoluble material was soluble in methylene chloride and yielded characteristic IR and ^1H NMR spectra. If an intermediate is proposed, and we will suppose for the time being that it forms reversibly, then the rate of disappearance of **2t** will depend on the rate of reaction of **I**. If the pathway toward soluble products (k_3) is much faster than reversal to **2t** (k_{-1}), then the rate constant for disappearance of **2t** will be k_1—that is, **I** will be "trapped" every time it forms. In the presence of PPh_3, the rate of disappearance of **2t** along the k_1 pathway will not be increased if $k_3 \gg k_{-1}$, since "saturation" kinetics apply even without the PPh_3. However, if $k_4[PPh_3]$ is comparable to k_3, then **I** will be diverted increasingly toward the phosphine-dependent k_4 pathway with increasing phosphine concentration until, in the limit of high phosphine concentration, no soluble products will form. At the same time as this k_4 pathway is giving **1-$PPh_3CH_3^+$** at the expense of the soluble products but without increasing the rate of disappearance of **2t**, a *bimolecular* phosphine-dependent pathway must be present to give the linear increase in rate of disappearance of **2t** with increasing phosphine concentration. This is the $k_2[PPh_3]$ reaction pathway and is assumed to be exactly analogous to that seen for the FeMn methoxycarbyne. As for the $k_4[PPh_3]$ pathway, the product of this reaction channel is assumed to be **1-$PPh_3CH_3^+$** since no soluble product is observed to be linearly dependent on $[PPh_3]$.

Application of the steady-state approximation to Scheme II gives in a straightforward manner the rate of decomposition of **2t** (eq 6), and rates of formation of products;

$$\frac{-d[\mathbf{2t}]}{dt} = \left(\frac{k_1}{k_{-1}/(k_3 + k_4L) + 1} + k_2L\right)[\mathbf{2t}] = (k_1 + k_2L)[\mathbf{2t}] \text{ for } (k_3 + k_4L) \gg k_{-1} \quad (6)$$

$$\text{yield}(\mathbf{1\text{-}PPh_3CH_3^+}) = \frac{d[\mathbf{1\text{-}PPh_3CH_3^+}]/dt}{-d[\mathbf{2t}]/dt} = \frac{k_1L/((k_3/k_4) + L) + k_2L}{k_1 + k_2L} \text{ for } (k_3 + k_4L) \gg k_{-1} \quad (7)$$

$$\text{yield(Fe or Cr)} = \frac{d[\text{Fe or Cr}]/dt}{-d[\mathbf{2t}]/dt} = \frac{k_1/(1 + (k_4/k_3)L)}{1 + (k_4/k_3)L} \text{ for } (k_3 + k_4L) \gg k_{-1} \quad (8)$$

L = $[PPh_3]$ for eqs 6–8;

Fe or Cr refers to total yields in Table III

the latter are converted to yields by dividing by the rate of disappearance of **2t**, as given in eq 7 for **1-$PPh_3CH_3^+$**

(23) Hersh, W. H.; Hunte, F.; Siegel, S. *Inorg. Chem.*, in press.

Scheme III

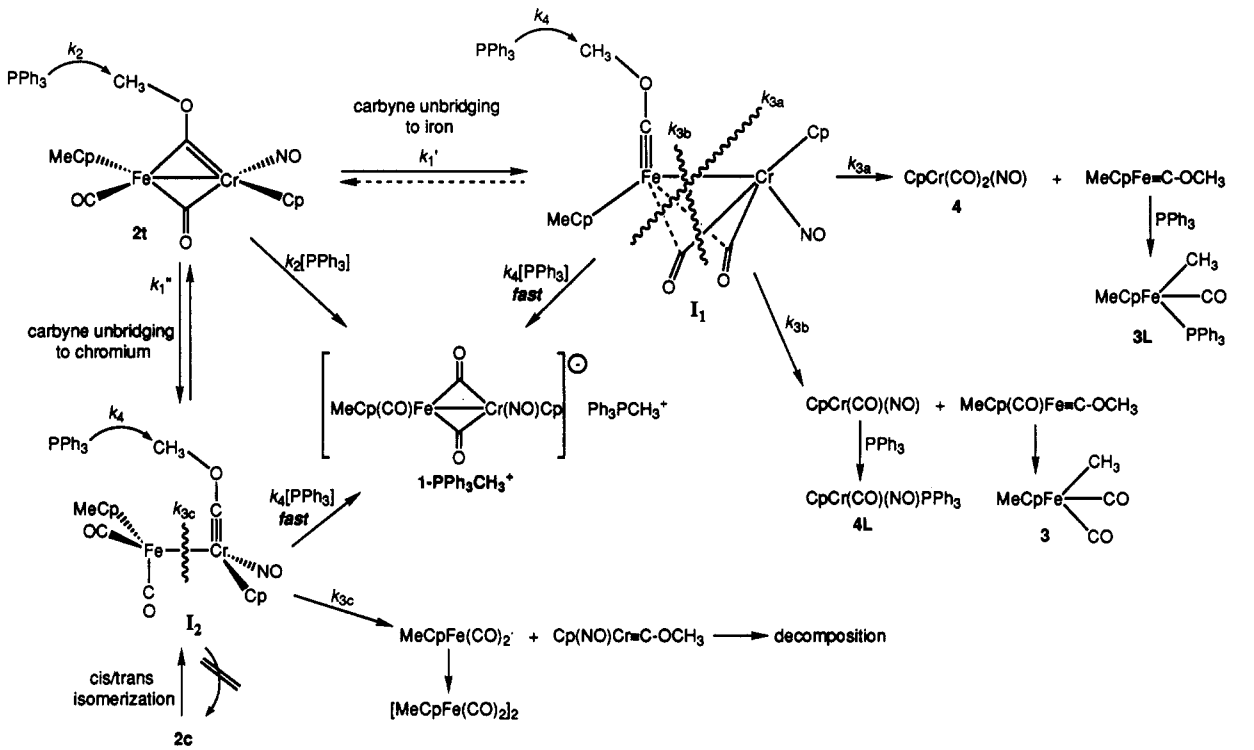

and in eq 8 for the soluble products. The rate equation for the disappearance of **2t** simplifies to give the observed rate law (eq 5) when $(k_3 + k_4L) \gg k_{-1}$, that is, when the intermediate **I** is trapped essentially every time it is formed. Since $k_{obs} = k_1$ in the absence of PPh_3, it must also be true that $k_3 \gg k_{-1}$, so in fact there is no evidence for reversibility in this reaction, save that the concentration of the intermediate cannot build up to detectable levels. The theoretical curves for the yields as a function of PPh_3 require that only one additional variable, k_4/k_3, be fit to the observed data, since the values for k_1 and k_2 are known from the least-squares fit in Figure 3 (and are given in eq 5). Values for k_4/k_3 were determined by assuming an initial value, calculating the theoretical yields for each concentration of PPh_3, and then varying k_4/k_3 to minimize a function of the differences between the theoretical and observed yields. The best value was determined by minimization of the sum of the square of the differences, each weighted by the reciprocal of the square of the deviation for each yield.[24] The theoretical curves in Figure 4 were generated using the value so obtained, $k_4/k_3 = 11.5$, and provide a reasonable fit to all the data. In order to generate an estimate of the error in k_4/k_3, the data were also fit using two other minimization functions. Thus, varying k_4/k_3 to minimize the sum of the square of the differences between the theoretical and observed yields, that is, without any weighting, gave $k_4/k_3 = 18.2$ and allowed an essentially perfect fit to the low concentration data where the yields change rapidly with $[PPh_3]$, but a poorer fit to the high concentration data where the yields level out. In order to more strongly weight the higher concentration points instead, the square of each difference was weighted by multiplying by the square of $[PPh_3]$. This function was minimized at $k_4/k_3 = 6.9$ and resulted in an excellent fit to the high concentration data but a relatively poor fit to the low concentration data. These latter two values for k_4/k_3 must be considered to represent outer limits, and adopting the average deviation from the overall best fit value above as an error estimate gives $k_4/k_3 = 11.5 \pm 5.7$. We conclude that the kinetic scheme given above allows the rate and yield data to be quantitatively fit using the two rate constants and one ratio of two rate constants shown in Scheme II.

A speculative proposed mechanism consistent with our results both for **2c** and **2t** as well as for the FeMn methoxycarbyne $MeCp(CO)Fe(\mu\text{-}COCH_3)(\mu\text{-}CO)Mn(CO)Cp$[2a] is shown in Scheme III; also included is a brief discussion of cis/trans isomerization. The simplest part of the mechanism is the bimolecular attack of PPh_3 directly on the methoxy methyl group of **2t**, indicated by k_2, to yield **1-$PPh_3CH_3^+$**. This S_N2 reaction is proposed to occur exactly as envisioned for the analogous reaction of the FeMn methoxycarbyne complex,[2a] with a negative charge formally ending up on chromium. The next part of the mechanism involves two competitive carbyne-unbridging pathways as shown to give I_1 with the terminal methoxycarbyne on iron and I_2 with the terminal carbyne on chromium. These pathways are considered in turn.

The formation of I_1 involves unbridging of the carbyne to give a terminal iron methoxycarbyne with concomitant bridging of the terminal Fe–CO ligand. While this might appear to involve a large degree of electron reorganization, in fact the carbyne bridge in **2** is likely to be nearly symmetrical with an M–C bond order of 1.5,[1b] so migration of the carbyne to either metal can be equally reasonable. The semi-bridging structure of I_1 is proposed by analogy to isoelectronic compounds such as $(\eta^5\text{-}Me_5C_5)(CO)Rh(\mu\text{-}CO)_2Mn(CO)Cp$[25]

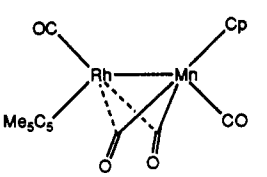

(24) Moore, J. W.; Pearson, R. G. *Kinetics and Mechanism*; 3rd ed.; Wiley-Interscience: New York, 1981; p 434.

and $Cp(PMe_3)Co(\mu\text{-}CO)_2Mn(CO)MeCp$[26] in which the 18-electron $CpMn(CO)_3$ unit is bound via semibridging carbonyl ligands to a 16-electron center ($Me_5C_5Rh(CO)$ or $CpCoPMe_3$). In $\mathbf{I}_1$, $CpCr(CO)_2NO$ takes the place of $CpMn(CO)_3$ and $MeCpFe{\equiv}COCH_3$ takes the place of $Me_5C_5Rh(CO)$. Breakdown of $\mathbf{I}_1$ along the k_{3a} pathway would be analogous to that seen by Werner,[26] in which ligand-induced decomposition gave $CpCo(PMe_3)L$ and $MeCpMn(CO)_3$. In the case of $\mathbf{I}_1$, unimolecular (rather than ligand-induced) decomposition gives $CpCr(CO)_2NO$ (**4**) and the 16-electron intermediate $MeCpFe{\equiv}COCH_3$, which either isomerizes to the more-familiar intermediate $MeCpFe(CO)CH_3$ which is trapped by PPh_3 or is first trapped by PPh_3 to give $MeCp(PPh_3)Fe{\equiv}COCH_3$ followed by isomerization, both to give **3L**. While the intermediacy of $MeCpFe{\equiv}COCH_3$ is certainly not required by the data, we have proposed that it is required for the Fe–Mn carbyne, where a 16-electron intermediate that is *not* $CpFe(CO)CH_3$ is involved in the reaction.[2a,23] Rather than propose unrelated mechanisms for the two carbynes, the terminal methoxycarbyne route is shown here, despite the fact that terminal methoxycarbynes are unknown and that even analogs of them are rare.[27] Breakdown of $\mathbf{I}_1$ along the k_{3b} pathway would allow direct formation of **3** (albeit via the 18-electron terminal methoxycarbyne intermediate $MeCp(CO)Fe{\equiv}COCH_3$) and **4L**. The k_{3a} and k_{3b} pathways are required since each of **3** and **3L** and **4** and **4L** must be a primary product of the decomposition of **2t** because interconversion does not occur under the reaction conditions.

At high PPh_3 concentration, the ratio of **3L**/**3** and **4**/**4L** tends toward ~80:20 (Table III)—the values at $[PPh_3]$ = 0.8 M are less reliable due to the small absolute amounts of each compound—suggesting that k_{3a} cleavage to give $MeCpFe{\equiv}COCH_3$ and **4** is ~4 times faster than the alternative k_{3b} cleavage to $MeCp(CO)Fe{\equiv}COCH_3$ and $CpCr(CO)(NO)$. At low PPh_3 concentration, the ratios are lower, and at $[PPh_3]$ = 0.01 M, *more* **4L** than **4** forms. One possible reason might be that other unsaturated fragments (such as $MeCpFe(CO)CH_3$) are less stable than $CpCr(CO)(NO)$ and so abstract CO from **4** faster than they are trapped by the low concentration of PPh_3. This would generate more of the 16-electron fragment that yields **4L** as well as more **3** as is in fact observed, although **3L** is still present in a greater amount than **3**. In the complete absence of phosphines, $\mathbf{I}_1$ would still be expected to undergo k_{3a} cleavage to give more 16-electron $MeCpFe{\equiv}COCH_3$ and **4** than $MeCp(CO)Fe{\equiv}COCH_3$ and 16-electron $CpCr(CO)NO$. However, the system is deficient in CO, and the low yield of **4** suggests that 16-electron $MeCpFe{\equiv}COCH_3$ or $MeCpFe(CO)CH_3$ must abstract CO from **4** to yield $CpCr(CO)(NO)$, which then decomposes, and that scavenging of CO is not efficient. In the reaction of the FeMn methoxycarbyne in the presence of 5 equiv of PPh_3, no $MeCpMn(CO)_2PPh_3$, the product that would be analogous to **4L**, formed nor did any $CpFe(CO)_2CH_3$, suggesting that the cleavage occurred in only one direction and that no subsequent CO abstraction by iron took place. There is no intuitively obvious reason for this result—for instance, it is not clear that $MeCpMn(CO)_2$ is particularly less stable than $CpCr(CO)(NO)$—but since the k_{3b} pathway is minor, it may be that the analogous pathway in the Mn system is only slightly more disfavored.

The formation of $\mathbf{I}_2$ involves concomitant unbridging of both the bridging ligands, as proposed for cis/trans isomerization of $[CpFe(CO)_2]_2$. In both cases, the resultant metal–metal single-bonded species can lead to cis/trans isomerization by rotation about the metal–metal bond followed by rebridging of the antiperiplanar ligands.[1b,5,8,28] Since isomerization of **2t** to **2c** is not observed, $\mathbf{I}_2$ effectively must be formed irreversibly from **2c**, a result which we presume is due to greater stability of the trans isomer. The barrier to conversion of **2c** to **2t** is high enough to allow their separation at room temperature, but it is unknown if the rate-determining step is unbridging or rotation about the metal–metal bond. Previously, we have discussed barriers to cis/trans isomerization in related compounds and noted that carbyne and isoelectronic nitrosyl ligands raise this barrier,[1b] and **2** has one of each. The molybdenum nitrosyl complex shown in the Introduction[3] also exhibits a high barrier to cis/trans isomerization, and so this and **2** both may represent examples of this nitrosyl ligand effect.

In addition to cis/trans isomerization, the intermediacy of $\mathbf{I}_2$ accounts in a natural way for the formation of $[MeCpFe(CO)_2]_2$, by simple homolytic cleavage along the k_{3c} pathway to give $MeCpFe(CO)_2$ which can then dimerize, as well as $CpCr(CO)(NO)CH_3$. Decomposition of this chromium alkyl could lead to **4** as well as **4L** via $CpCr(CO)(NO)$, and these products must form in the k_{3c} step in order to give the observed yields. That is, we have assumed above that the iron dimer forms in the overall k_3 step, an assumption justified by the fit of the yield data to the total of the *three* iron products as well as to the two chromium products, but this requires that some **4** and/or **4L** form in the iron dimer-producing step. As noted above, roughly half of the methyl group not tied up by **1-$PPh_3CH_3^+$** is lost during the reaction, and while we cannot account for it, it is reasonable to propose that it is lost at this point. The yield of $[MeCpFe(CO)_2]_2$ is in accord with this proposal, since it roughly parallels that of the iron alkyls **3** and **3L**. That is, the k_{3c} path, where the dimer forms and the CH_3 group is proposed to be lost, is comparable to the sum of the k_{3a} and k_{3b} pathways, where **3** and **3L** form, which would give the observed extent of CH_3 group loss.

Lastly, the kinetic analysis requires rapid trapping of an intermediate by PPh_3 along the k_4 pathway to give back **1-$PPh_3CH_3^+$**. Since two intermediates are proposed, both must be trapped as shown. As noted above, since the k_{3c} pathway is comparable to the sum of the k_{3a} and k_{3b} pathways, each of $\mathbf{I}_1$ and $\mathbf{I}_2$ is required by the product yield data to give **1-$PPh_3CH_3^+$** by the k_4 pathways. While this feature of the mechanism is inelegant, particularly since the kinetic data was accounted for by a single

(25) Aldridge, M. L.; Green, M.; Howard, J. A. K.; Pain, G. N.; Porter, S. J.; Stone, F. G. A.; Woodward, P. *J. Chem. Soc., Dalton Trans.* **1982**, 1333–1340.

(26) (a) Leonhard, K.; Werner, H. *Angew. Chem., Int. Ed. Engl.* **1977**, *16*, 649–650. (b) Werner, H.; Juthani, B. *J. Organomet. Chem.* **1981**, *209*, 211–218. (c) Werner, H. *Pure Appl. Chem.* **1982**, *54*, 177–188.

(27) Examples include aryloxycarbynes (a), siloxycarbynes (b,c), thiocarbynes (d–g), and a proposed alkoxycarbyne intermediate (h,i): (a) Jamison, G. M.; White, P. S.; Templeton, J. L. *Organometallics* **1991**, *10*, 1954–1959. (b) Vrtis, R. N.; Liu, S.; Rao, C. P.; Bott, S. G.; Lippard, S. J. *Ibid.* **1991**, *10*, 275–285. (c) Vrtis, R. N.; Bott, S. G.; Lippard, S. J. *Ibid.* **1992**, *11*, 270–277. (d) Dombek, B. D.; Angelici, R. J. *Inorg. Chem.* **1976**, *15*, 2397–2402. (e) Greaves, W. W.; Angelici, R. J. *Ibid.* **1981**, *20*, 2983–2988. (f) Fortune, J.; Manning, A. R. *Organometallics* **1983**, *2*, 1719–1723. (g) Kim, H. P.; Angelici, R. J. In *Advances in Organometallic Chemistry*; Stone, F. G. A., West, R., Eds.; Academic Press: San Diego, 1987; Vol. 27; pp 51–111. (h) Schubert, U.; Hörnig, H. *J. Organomet. Chem.* **1987**, *336*, 307–315. (i) Schubert, U. *Ibid.* **1988**, *358*, 215–228.

(28) Farrugia, L. J.; Mustoo, L. *Organometallics* **1992**, *11*, 2941–2944.

intermediate, the two intermediates are necessary to account for the complex product mixture, and the k_1 pathway is really made up of $k_1 = k_1' + k_1''$. The reactions of the FeMn methoxycarbyne were also proposed to proceed via two intermediates, but the differences were that no decomposition of the $\mathbf{I_2}$ analog was necessary, only one decomposition pathway (k_{3a}) was necessary for the $\mathbf{I_1}$ analog, and there was no kinetic evidence for the conversion of the intermediates back to **1-$PPh_3CH_3^+$** by the k_4 pathway. The added complexities of the FeCr methoxycarbyne may arise due to its higher reactivity, evidence of which is provided by $k_1 = 6.5 \times 10^{-4}$ s^{-1} at 50 °C compared to the lower value of $k_1 = 1 \times 10^{-4}$ s^{-1} at the higher temperature of 75 °C for the FeMn methoxycarbyne.[2a]

Conclusions

We have described the high-yield synthesis and X-ray structure of a novel heterodinuclear iron–chromium anion, a member of the well-known $[CpFe(CO)_2]_2$ "iron dimer" structural class of compounds. This anion, which contains a strong π-acid nitrosyl ligand, appears to be a relatively poor nucleophile, and alkylation to give the novel methoxycarbynes **2c** and **2t** occurs in low yield. Kinetic investigations of thermal reactions of the trans isomer were carried out and show that the methyl migration reaction of this carbyne is exceptionally complicated. In the absence of PPh_3, apparent oxygen to iron methyl migration occurs along with metal–metal bond cleavage to give the iron alkyl $MeCpFe(CO)_2CH_3$ and $CpCr(CO)_2NO$, but in this reaction more than half of the methyl group cannot be accounted for. In the presence of PPh_3, $MeCpFe(CO)(PPh_3)CH_3$ and $CpCr(CO)(NO)PPh_3$ also form, and in addition a bimolecular pathway operates in which dealkylation of the carbyne methyl group occurs to give back the $Ph_3PCH_3^+$ salt of the FeCr anion. However, the bimolecular pathway cannot account for the decrease in yields of soluble products with increasing PPh_3 concentration, which asymptotically approach zero. Incorporation into the mechanism of a common intermediate that can be drained off to give additional $Ph_3PCH_3^+$ salt of the FeCr anion at the expense of the soluble products, *without increasing the rate of unimolecular carbyne decomposition*, allows both the unusual yield and rate data to be quantitatively explained. Further complications include the formation of both $MeCpFe(CO)(PPh_3)CH_3$ and $CpCr(CO)_2NO$ (the major decomposition products) and $MeCpFe(CO)_2CH_3$ and $CpCr(CO)(NO)PPh_3$ (the minor decomposition products), suggesting that two modes of carbyne cleavage occur from the common intermediate. The formation of comparable amounts of $[MeCpFe(CO)_2]_2$ suggests yet another mode of carbyne cleavage. We are in fact unable to construct a single intermediate that can reasonably yield all of these products and so propose two intermediates, one in which the methoxycarbyne is bound in terminal fashion to iron and the other to chromium. Similar intermediates have been proposed for the related iron–manganese methoxycarbyne complex, but the product mixture was less complicated in that case, perhaps due to its lower reactivity. While the rich array of reaction channels observed here allows the possibility of generating new insight into the mechanism of methoxycarbyne decomposition and methyl migration, further work on this particular iron–chromium system is not anticipated due to the low yield. Future work will focus on the analogous molybdenum or tungsten systems in anticipation of higher yields of products that may shed light on these surprisingly complicated results.

Experimental Section

General. All manipulations of air-sensitive compounds were carried out either in a Vacuum Atmospheres inert atmosphere drybox under recirculating nitrogen or by using standard Schlenk techniques. ^{1}H NMR spectra were recorded on an IBM/Bruker WP-200SY spectrometer, and except as noted ^{13}C NMR spectra were recorded on a JEOL GX400 spectrometer operating at 100.4 MHz; chemical shifts are reported relative to TMS or hydrogen in C_6D_6 (δ 7.15), CD_2Cl_2 (δ 5.32), acetone-d_6 (δ 2.04), or CD_3CN (δ 1.93) and to toluene-d_8 at 20.4 ppm or acetone-d_6 at 29.8 ppm for ^{13}C NMR. Infrared spectra were obtained on a Mattson Galaxy 4020 FT-IR spectrometer with 0.1-mm NaCl solution cells. Elemental analyses were performed by Desert Analytics, Tucson, AZ. Mass spectra (EI) were obtained on a HP5988A spectrometer. Photolyses were carried out with a medium-pressure 450-W mercury Hanovia lamp.

All solvents were treated under nitrogen. Acetonitrile was purified by sequential distillation from calcium hydride and phosphorus pentoxide. Benzene, diethyl ether, and tetrahydrofuran were distilled from sodium benzophenone ketyl. Hexane was purified by washing successively with 5% nitric acid in sulfuric acid, water, sodium bicarbonate solution, and water and then dried over calcium chloride and distilled from *n*-butyllithium in hexane. Pentane was dried over 3-Å sieves and vacuum-transferred. Methylene chloride was distilled from phosphorus pentoxide; CD_2Cl_2 was vacuum-transferred from phosphorus pentoxide. Acetone-d_6 and CD_3CN were dried over 4-Å molecular sieves and vacuum-transferred prior to use; benzene-d_6 and toluene-d_8 were vacuum-transferred from sodium benzophenone ketyl.

Silica gel (200–400 mesh) was dried for several hours under vacuum while heating with a heat gun and was transferred under vacuum into the drybox. Triphenylphosphine was recrystallized from ethanol, and methyl triflate (Aldrich) and TMS were vacuum-transferred from CaH_2. $Me_3O^+BF_4^-$ (Lancaster), Ph_2PMe (Pressure Chemical), and $Ph_3PCH_3^+Br^-$ (Aldrich) were used as received. $CpCr(CO)_2NO$ was prepared by the published procedure,[29] and $MeCpFe(CO)_2^-Na^+$ was prepared as previously described.[1b]

$[MeCp(CO)Fe(\mu\text{-}CO)_2Cr(NO)Cp]^-Na^+$ (1). Although the synthesis of CpCr(CO(NO)THF has been described, details of our procedure are given due to the variability of this reaction. In the glovebox, 2.46 g (12.11 mmol) of $CpCr(CO)_2NO$ was placed in a 1-L round-bottom flask equipped with a magnetic stirrer, 650 mL of THF was added, and the flask was capped with a rubber septum. The mixture was placed in an ice-cooled water bath and irradiated using a 450-W Hanovia medium-pressure mercury lamp, with nitrogen bubbling through the solution via a long syringe needle and exiting via another syringe needle attached to an oil bubbler. The orange solution was photolyzed until no more changes ($CpCr(CO)_2NO$: 2017 (m), 1945 (m), 1699 (m) cm^{-1}; CpCr(CO)(NO)(THF): 1904 (m), 1642 (m) cm^{-1}) were observed in the IR, typically about 1.5–2 h; the color was black-brown. The bands due to the starting material at 2017 and 1699 cm^{-1} were slightly less intense, while that at 1945 cm^{-1} was slightly more intense, than those due to the product. A solution of 2.80 g of $MeCpFe(CO)_2^-Na^+\cdot(THF)_{\sim 0.5}$ (11.20 mmol) in 90 mL of THF was added via syringe, and the solution was vigorously stirred for 2.5 h, at which point no CpCr(CO)(NO)(THF) or $MeCpFe(CO)_2^-$ remained. Under a strong flow of nitrogen, the septum was replaced by a vacuum stopcock, and the solvent was removed on a vacuum line. In the glovebox, 100 mL of benzene was added to the black residue and the suspension stirred for 0.5 h. The mixture was then filtered on a coarse frit and the solid collected was washed with three 50-mL portions of benzene to remove

(29) Hoyano, J. K.; Legzdins, P.; Malito, J. T. *Inorg. Synth.* **1978**, *18*, 126–129.

$CpCr(CO)_2NO$ and $[MeCpFe(CO)_2]_2$, until the filtrate was colorless. The solid was dried for 2 h to give 2.78 g (59% yield based on chromium) of a brown-black solid. The combined filtrates were generally stripped of solvent and the residue subjected to vacuum sublimation (~30–35 °C, ~0.1 mmHg); $CpCr(CO)_2NO$ was recovered in 30% yield: IR (THF) 1894 (s), 1746 (m), 1718 (s), 1672 (m), 1597 (m), 1557 (m) cm^{-1}; IR (CH_3CN) 1891 (m), 1729 (w, sh), 1698 (s), 1581 (m) cm^{-1}; ^1H NMR (CD_3CN) δ 4.65 (br s, 5 H, Cp), 4.41 (br s, 1 H, Me*Cp*), 4.17 (br s, 3 H, Me*Cp*), 1.76 (br s, 3 H, *Me*Cp).

$[MeCp(CO)Fe(\mu\text{-}CO)_2Cr(NO)Cp]^-PPN^+$ (1-PPN^+). In the glovebox 60 mL of THF was added to 823 mg of **1** (2.12 mmol) and 1.22 g of PPN^+Cl^- ($PPN^+ = (Ph_3P)_2N^+$)[30] (2.13 mmol) and the resulting mixture stirred vigorously for 15 min. The mixture was then filtered through a medium frit and the solid washed with THF until the rinses were nearly colorless. The THF was removed from the filtrate on the vacuum line, the residue was redissolved in 30 mL of CH_3CN and filtered through a coarse frit, and finally 20 mL of ether was carefully layered on top of the CH_3CN solution. The mixture was then stored in the glovebox freezer (−40 °C) for at least 3 days, but this particular preparation was allowed to stand for ~1 month. After the resultant solid was filtered and washed with ether, 785 mg (41% yield) of fine black crystals was obtained. Samples for elemental analysis and X-ray diffraction were obtained by dissolving the crystalline material in the minimum amount of acetonitrile, filtering, and cooling to −40 °C overnight. The resultant blocky crystals (~30% recovery) were washed with ether: IR (THF) 1885 (m), 1738 (w), 1709 (s), 1590 (m) cm^{-1}; (CH_3CN) 1891 (m), 1730 (w), 1698 (s), 1588 (m) cm^{-1}; (CH_2Cl_2) 1891 (m), 1725 (w), 1692 (s), 1574 (m) cm^{-1}; ^1H NMR (acetone-d_6) δ 7.71, 7.59 (m, 30 H), 4.58 (s, 5 H, Cp), 4.37 (m, 2 H, Me*Cp*), 4.12 (m, 2 H, Me*Cp*), 1.79 (s, 3 H, *Me*Cp); (CD_3CN) δ 7.62, 7.51 (m, 30 H), 4.64 (br s, 5 H, Cp), 4.41 (br s, 2 H, Me*Cp*), 4.16 (s (less broad than 4.64, 4.41), 2 H, Me*Cp*), 1.77 (br s, 3 H, *Me*Cp); (CD_2Cl_2) δ 7.66, 7.50 (m, 30 H), 4.70 (s, 5 H, Cp), 4.48 (s, 2 H, Me*Cp*), 4.22 (s, 2 H, Me*Cp*), 1.76 (s, 3 H, *Me*Cp); ^{13}C NMR (acetone-d_6, −48 °C) 320.11 (μ-CO), 214.70 (FeCO), PPN^+ at 134.33 (C_4), 132.90, 130.17 (C_2, C_3), and 127.82 (d, J_{PC} = 106.7 Hz, C_1), 102.37 (η^5-$CH_3CC_4H_4$), 93.87 (*Cp*Cr), 87.43, 86.22 (η^5-$CH_3CC_4H_4$), 13.08 (η^5-$CH_3CC_4H_4$) ppm. Anal. Calcd for $C_{50}H_{42}N_2O_4PCrFe$: C, 66.38; H, 4.68; N, 3.10. Found: C, 66.27; H, 4.57; N, 3.10.

$[MeCp(CO)Fe(\mu\text{-}CO)_2Cr(NO)Cp]^-Ph_3PCH_3^+$ (1-$Ph_3PCH_3^+$). In the glovebox, 100 mL of THF was added to 304 mg of **1** (0.78 mmol) and 308 mg of $Ph_3PCH_3^+Br^-$ (0.86 mmol) and the resulting mixture stirred vigorously for 5 min. The mixture was filtered through a coarse frit and the solid washed with three 20-mL portions of THF, at which point the wash was nearly colorless. The solvent was removed on a vacuum line and redissolved in 30 mL of CH_3CN back in the glovebox. The solution was filtered through a medium frit and concentrated to ~10 mL. Ether (~10 mL) was layered on top of the acetonitrile, and the mixture was stored at −40 °C for 2 days. The resultant black crystals were filtered and washed with ether to give 350 mg of product (70% yield). Samples for elemental analysis and X-ray diffraction were obtained by dissolving the crystalline material (45 mg) in 2 mL of CH_3CN, layering on 2 mL of ether, and storing at −40 °C overnight; the resultant blocky crystals (32 mg) were washed with ether: IR (CH_2Cl_2) 1894 (m), 1725 (w), 1690 (s), 1572 (m) cm^{-1}; ^1H NMR (CD_2Cl_2) 7.75 (m, 15 H), 4.75, 4.65 (br s, 5 H, minor and major Cp), 4.43 (br s, ~1.5 H, Me*Cp*), 4.19 (br s, ~2 H, Me*Cp*), 4.05 (br s, ~0.5 H, Me*Cp*), 2.85 (d, 3 H, J_{PH} = 13 Hz, Ph_3PCH_3), 1.96, 1.74 (br s, 3 H, minor and major *Me*Cp, 30:70). Anal. Calcd for $C_{33}H_{30}NO_4PCrFe$: C, 61.60; H, 4.70; N, 2.18. Found: C, 61.56; H, 4.75; N, 2.03.

***cis*- and *trans*-MeCp(CO)Fe(μ-$COCH_3$)(μ-CO)Cr(NO)Cp (2c, 2t).** In the glovebox, 955 mg of **1** (2.45 mmol) and 474 mg of $Me_3O^+BF_4^-$ (3.20 mmol) were dissolved in 25 mL of CH_3CN. The dark solution was stirred vigorously for 3 min, and then the solvent was removed on a vacuum line to give 1.295 g of a dark red-brown oil. To this residue was added 50 mL benzene, and the mixture was stirred for 1 h. The mixture was filtered though a coarse frit to give 457 mg of a dark brown powder; 80 mg of this material was soluble in CH_2Cl_2 but had no CO or NO bands in the IR spectrum. A 100% recovery of $NaBF_4$ could account for 269 mg of the remaining benzene- and CH_2Cl_2-insoluble material. The benzene was removed from the filtrate on the vacuum line to give 794 mg of an oily black-red residue. This material was applied (in CH_2Cl_2) to a 2.2 × 33 cm silica gel chromatography column packed in hexane, in the glove box. Elution with hexane gave a trace of unidentified green material in the first 100-mL fraction. The column was then eluted with 4:1 hexane/diethyl ether, giving $CpCr(CO)_2NO$ (~10 mg) in a second orange band in a 30-mL fraction, $[MeCpFe(CO)_2]_2$ (300 mg, 64% yield) in a dark red third band in a 100 mL fraction, and **2t** (90 mg of red-brown powder, 9.6% yield) in a dark red fourth band in a 100 mL fraction. Elution was continued with 1:1 hexane/diethyl ether, giving a trace of unidentified material in a fifth green band in 120 mL and **2c** (89 mg of brown powder, 9.5% yield) in a sixth lighter red band in 180 mL. Elution with ether then gave a seventh orange-red band containing ~20 mg of compound identified as $CpCr(CO)(NO)(CH_3CN)$ (IR (THF) 1916 (s), 1650 (s) cm^{-1}; ^1H NMR (C_6D_6) δ 4.69 (s, 5 H), 0.36 (s, 3 H)), and finally elution with THF gave ~30 mg of uncharacterized black-brown material in a 70 mL fraction; an immobile black band remained at the top of the column. Attempts to crystallize **2t** from pentane, hexane, or ether failed due to its high solubility, but material that contained ~5% $[MeCpFe(CO)_2]_2$ (as judged by ^1H NMR) was reproducibly obtained from the chromatography and was directly used for all further experiments. Crystallization of **2c** was best accomplished by layering pentane onto a $CHCl_3$ solution of **2c** and cooling overnight at −40 °C to give spectroscopically, although not analytically, pure material as black crystals. Five elemental analyses with material crystallized from various combinations of CH_2Cl_2, ether, hexane, and toluene (in addition to the above mixture) were carried out; the values shown below are typical and come from a CH_2Cl_2/ether crystallization. The low carbon analyses for both carbynes are ascribed to thermal decomposition. **2t**: IR (C_6H_6) 1945 (s), 1795 (m), 1650 (s) cm^{-1}; ^1H NMR (C_6D_6) δ 4.72 (s, 5 H, Cp), 4.56 (m, 1 H, Me*Cp*), 4.45 (m, 2 H, Me*Cp*), 4.28 (s, 4 H, Me*Cp* (1 H) overlapping MeO), 1.62 (s, 3 H, *Me*Cp); ^{13}C NMR (toluene-d_8, 0 °C) 428.32 (μ-$COCH_3$), 290.8 (μ-CO, $\Delta\nu$ = 130 Hz), 213.01 (FeCO), 105.32 (η^5-$CH_3CC_4H_4$), 95.15 (CpCr), 89.68, 88.23, 87.74, 86.86 (η^5-$CH_3CC_4H_4$), 72.86 (μ-$COCH_3$), 12.54 ($CH_3CC_4H_4$). Anal. Calcd for $C_{15}H_{15}NO_4CrFe$: C, 47.27; H, 3.97; N, 3.68. Found: C, 42.33; H, 3.64; N, 3.33. **2c**: IR (C_6H_6) 1966 (s), 1794 (m), 1659 (s) cm^{-1}; ^1H NMR (C_6D_6) δ 4.62 (s, 5 H, Cp), 4.29 (s, 3 H, MeO), 4.22, 4.03, 3.83, 3.77 (m, 1 H each, Me*Cp*), 1.72 (s, 3 H); ^{13}C NMR (toluene-d_8, 0 °C) 427.62 (μ-$COCH_3$), 289.5 (μ-CO), 211.03 (FeCO), 103.16 (η^5-$CH_3CC_4H_4$), 94.05 (CpCr), 87.86, 86.98, 85.13, 84.92 (η^5-$CH_3CC_4H_4$), 73.32 (μ-$COCH_3$), 12.84

Table V. Crystallographic Data for Structure 1

formula	$C_{33}H_{30}CrFeNO_4P$
fw	643.42
space group	$P2_1/n$
cryst system	monoclinic
a, Å	9.276(2)
b, Å	14.925(3)
c, Å	21.875(4)
β, deg	102.60(5)
V, Å^3	2955.5(10)
Z	4
d_{calc}, g cm^{-3}	1.446
μ, cm^{-1}	9.51
radiation (λ, Å)	Mo Kα (0.710 73)
scan type	ω
2θ range	4–55°
reflns collected	7328
indept reflns	6774
obsd reflns ($F_o > 4\sigma(F_o)$)	4478
largest diff peak, e Å^{-3}	0.32
largest diff hole, e Å^{-3}	−0.31
R, R_w	0.043, 0.052
data/parameter	12.1

(30) Ruff, J. K.; Schlientz, W. J. *Inorg. Synth.* **1974**, *15*, 84–90.

($CH_3CC_4H_4$). Anal. Calcd for $C_{15}H_{15}NO_4CrFe$: C, 47.27; H, 3.97; N, 3.68. Found: C, 45.67; H, 3.91; N, 3.35.

Crystallographic Structural Determination. Crystal data for 1-$Ph_3PCH_3^+$ are given in Table V. The dark red crystal rods (0.30 × 0.40 × 0.50 mm) were obtained from CH_3CN/ether as described above and were mounted on a glass fiber. Data were collected on a Siemens *P*4 diffractometer with graphite monochromator at room temperature. No correction for absorption was required ($T_{max}/T_{min} < 1.1$). The structure was solved by direct methods (TREF). The structure was refined using full-matrix, least-squares techniques. All non-hydrogen atoms were refined anisotropically, and all hydrogen atoms were fixed at idealized positions. All computations used SHELXTL software (Sheldrick, Siemens, Madison, WI).

^{1}H NMR Experiments. General. In the glovebox, solid PPh_3 (for the reactions in which it was used) was loaded into an NMR tube sealed to a 14/20 ground glass joint, while the carbyne was dissolved in a small amount of C_6D_6 and transferred and rinsed into the tube. TMS (~1 μL) was added by a microliter syringe. Benzene-d_6 was added to a height of ~3.5 cm, a vacuum stopcock was fitted to the tube, and the tube was attached to a vacuum line. The tube was submitted to three freeze–pump–thaw cycles and sealed with a torch. Heating was carried out by inverting the tube in a thermostatted water bath; samples were quenched by immersing in an ice bath, and the tube was centrifuged prior to recording each NMR spectrum. The volume was calculated according to the equation $V = \pi(0.213)^2h$, where h is the height of the solvent measured immediately after removal from the hot bath.

Identification of all products was carried out by ^{1}H NMR; chemical shifts in C_6D_6 are as follows. **MeCpFe(CO)$_2$CH$_3$**:[31] δ 3.99 (m, 2 H), 3.85 (m, 2 H), 1.36 (s, 3 H), 0.30 (s, 3 H). **MeCpFe(CO)(PPh$_3$)CH$_3$**:[11] δ 4.07 (m, 2 H), 3.84 (m, 1 H), 3.71 (m, 1 H), 1.69 (s, 3 H), 0.27 (d, J_{PH} = 6.7 Hz). **[MeCpFe(CO)$_2$]$_2$**:[31b] δ 4.17 (m, 2 H), 4.05 (m, 2 H), 1.72 (s, 3 H). **CpCr(CO)$_2$(NO)**:[29] δ 4.22 (s). **CpCr(CO)(NO)PPh$_3$**:[10] δ 4.45 (d, J_{PH} = 2 Hz). **CH$_4$**: δ 0.15.

^{13}C NMR of CpCr(CO)$_2$NO. For comparison to the spectra of the Fe–Cr compounds, the ^{13}C NMR spectrum (50 MHz) of $CpCr(CO)_2NO$ was recorded in acetone-d_6 in the presence of ~0.05 M $Cr(acac)_3$,[8a] giving sharp peaks at 238.6 and 91.8 ppm.

Isolation of 1-$Ph_3PCH_3^+$ from PPh_3 Reaction of 2t. A sample of **2t** (5.0 mg, 0.013 mmol) and PPh_3 (65.5 mg, 19 equiv, 0.49 M) in C_6D_6 was prepared as described above and heated at 50 °C for 10.7 h. Inspection by ^{1}H NMR showed that all of the carbyne had decomposed, and a large amount of precipitate was present. In the glovebox, the tube was broken, and the contents were filtered through a frit and washed with C_6D_6 until the washes were colorless. The resultant black-brown crystals were dried, giving 12 mg (142% yield) of product (possibly contaminated by ~3.5 mg of PPh_3) that was completely soluble in CD_2Cl_2 and whose IR and ^{1}H NMR were identical to those of 1-$Ph_3PCH_3^+$.

Acknowledgment. Financial support for this work from the National Science Foundation (CHE-9096105) is gratefully acknowledged.

Supplementary Material Available: Tables of crystallographic data for 1-$Ph_3PCH_3^+$ (8 pages). Ordering information is given on any current masthead page.

OM920720H

(31) (a) Piper, T. S.; Wilkinson, G. *J. Inorg. Nucl. Chem.* **1956**, *3*, 104–124. (b) King, R. B. *Organometallic Syntheses, Vol. 1: Transition-Metal Compounds*; Academic Press: New York, 1965; Vol. 1, pp 151–152.